Energy Conversion and Management 53 (2011) 135–141

Contents lists available at SciVerse ScienceDirect

Energy Conversion and Management

journal homepage: www.elsevier.com/locate/enconman

Experimental and computational studies on a gasifier based stove

S. Varunkumar *, N.K.S. Rajan, H.S. Mukunda

Combustion, Gasification and Propulsion Laboratory, Department of Aerospace Engineering, Indian Institute of Science, Bangalore 560 012, India

ARTICLE INFO

Article history:
Received 18 July 2011
Received in revised form 30 August 2011
Accepted 31 August 2011
Available online xxxx

Keywords:
Gasifier stove
Biomass combustion
Gasification efficiency

ABSTRACT

The work reported here is concerned with a detailed thermochemical evaluation of the flaming mode behaviour of a gasifier based stove. Determination of the gas composition over the fuel bed, surface and gas temperatures in the gasification process constitute principal experimental features. A simple atomic balance for the gasification reaction combined with the gas composition from the experiments is used to determine the CH_4 equivalent of higher hydrocarbons and the gasification efficiency (η_g). The components of utilization efficiency, namely, gasification–combustion and heat transfer are explored. Reactive flow computational studies using the measured gas composition over the fuel bed are used to simulate the thermochemical flow field and heat transfer to the vessel; hither-to-ignored vessel size effects in the extraction of heat from the stove are established clearly. The overall flaming mode efficiency of the stove is 50–54%; the convective and radiative components of heat transfer are established to be 45–47 and 5–7% respectively. The efficiency estimates from reacting computational fluid dynamics (RCFD) compare well with experiments.

1. Introduction

A stove design that ensures near-stoichiometric operation to maximize efficiency and minimize emissions, limits the velocities in the fuel residing zone to limit particle carry-over with vessels of practical relevance was evolved using principles of gasifier with air supply from a fan [1–4]. Gasification is one of the predominant routes for conversion of biomass to energy (see for instance [5,6]). This stove design was engineered using the principles of gasification into a commercial product and sold commercially to half-a-million house holds along with agriculture residue based pellet fuel. This stove assures an utilization efficiency of over 50% and CO emission of 0.75 g/MJ of heat input. Compared to stoves based on air supply by natural convection, these efficiencies are 40–60% higher and CO emissions about 50–70% lower. Pushing the understanding to the next level, where the thermochemical processes are examined in detail may allow further optimization of efficiency and emissions. One important feature guiding these developments is that efficiency and emissions have an inverse correlation – higher efficiency obtained by better combustion allows for lowering the emissions.

There are several earlier studies on packed bed gasification and combustion [5–11]. Most of these studies have been restricted to high air flow rate (superficial velocity >8 cm/s) regimes which find application in large scale combustion in power generation systems. Work of Reed and colleagues [3,12] is probably the only one which addresses the problem of thermochemical processes in the superficial velocity range of 3–6 cm/s, a range of particular interest to small clean combustion devices of focus in this paper. Current work goes beyond the work of Reed and colleagues by addressing the crucial gas phase processes affecting the various components of efficiency.

This stove shown in Fig. 1 has a combustion space of 100 mm diameter and 130 mm depth with a grate in the bottom and wood chips or pellets of biomass can be used as fuel. The stove is a top-lit downdraft gasifier (see [13]) with air for gasification (primary air) provided from the bottom region and the gas generated in the process of gasification burnt on top with secondary air to ensure complete combustion and minimum emissions. Domestic cooking requires power in the range of 3–4 kWth and this corresponds to a biomass consumption of 10–15 g/min. This requires a primary air flow rate in the range of 15–25 g/min for 100 mm diameter stove; the superficial velocity, a key parameter for obtaining optimal gas quality [12] corresponding to this range is 3–6 cm/s. When the stove is loaded with biomass and is lit on top by sprinkling small amounts of liquid fuel (say, alcohol or kerosene), de-volatilisation of biomass leads to ignition of particles in the top most layer. This in turn leads to similar processes in the subsequent layers of biomass particles. This flame front propagates into the fuel bed against the air stream similar to a premixed flame propagation in a tube, albeit with heterogeneous local fuel source. The air that passes from the bottom through the bed aids flaming combustion of the biomass pieces and the gases move upward through the hot char bed left behind by the propagating pyrolysis front. This leads

* Corresponding author. Tel.: +91 80 23600536; fax: +91 80 23601692.
E-mail addresses: varun@cgpl.iisc.ernet.in (S. Varunkumar), nksr@cgpl.iisc.ernet.in (N.K.S. Rajan), mukunda@cgpl.iisc.ernet.in (H.S. Mukunda).

0196-8904/$ - see front matter © 2011 Elsevier Ltd. All rights reserved.
doi:10.1016/j.enconman.2011.08.022

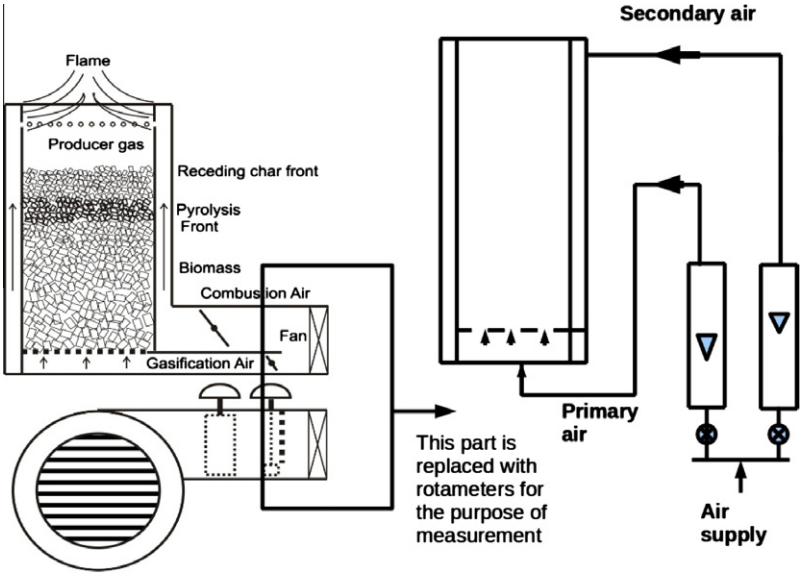

Fig. 1. Schematic of a gasifier stove with the gasification air flowing from bottom to top and another stream of air through radial holes at the top helps combustion of the combustible gases; the part on the right is the modification for the current experiments to help control the air flow rates.

to reduction reactions and the gases that issue from the top region are fuel rich. Secondary air from the top mixes and burns with this combustible gas ensuring complete combustion with minimum emissions and maximum possible heat transfer to the vessel.

The efficiency of the stove in these modes at different equivalence ratios are experimentally determined and reported in [14]. The major conclusion of [14] are: (a) the gasification A/F is 1.5 in the operation regime of the stove (b) the maximum overall efficiency of the stove is 52% and occurs close to stoichiometric operating point; (c) the flaming mode contributes 45% and the char mode contributes 7% to the overall efficiency; (d) 60% of the total CO emissions come from the char mode with only 20% of the total energy consumption; (e) drastic changes in A/F during the transition to char mode combined with secondary air cooling effect is shown to be the reason for low char mode efficiency and ways to improve the char mode efficiency from 7% to 20% are brought out; with this improvement the total CO emissions came down by 50%; the insights obtained were used to improve the efficiency of the existing commercial design by more than 5%.

1.1. Flaming and char mode

There are two phases in the consumption of the biomass (see Fig. 2). The first phase involves the evolution of volatile gases and conversion of the biomass to char by the propagating pyrolysis front. This referred to as the *flaming mode* [15]. Once the front reaches the grate, all biomass is de-volatilised and about 20% of hot char is left on the grate. The air coming in through the grate causes surface oxidation of char and generates primarily CO and CO_2 and little H_2. CO_2 so generated passes through the hot char on top and can undergo reduction with carbon to form CO. The conversion process in the char mode is also gasification till the last 5% burn time. After this, the amount of char left behind is consumed in a combustion mode and what will be left behind finally is ash [16]. This is referred to as the *char mode*. The power levels are 3 ± 0.5 kW in flaming and 0.5 ± 0.1 kW in char modes. Mass, energy and power levels in the two modes are shown in Table 1. It is clear that flaming mode constituted 80% of the total energy consumption and this work is concerned with detailed thermochemical evaluation of flaming mode using computations and experiments.

The paper is organised as follows: (1) Gas composition and gasification efficiency, (2) Simulation of gas phase combustion and heat transfer, (3) Radiation heat transfer efficiency, (4) Concluding remarks.

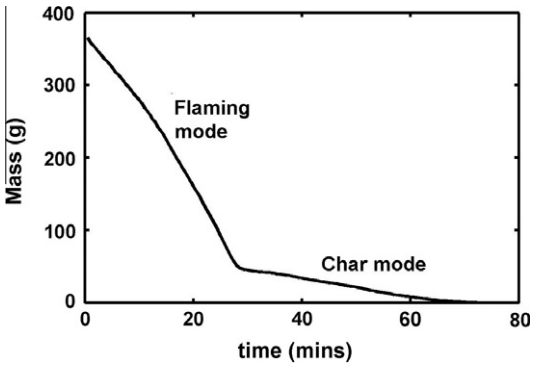

Fig. 2. Mass loss vs. time for wood.

2. Gas composition and gasification efficiency (η_g)

The schematic of the experiment in shown in Fig. 3. The stove is 100 mm dia 130 mm long cylindrical chamber with a grate at the bottom, conforming to the actual commercialized design. Air for gasification comes from the bottom and for combustion of gasification products is supplied on top of the bed from 18 holes of 5 mm dia each. The air flow rates are controlled with a calibrated variable area rotameters. The stove was loaded with about 400 g of wood pieces 10–15 mm size and placed on a balance (0.5 g precision) to enable continuous mass measurement during the test. The ignition process involved placing some kerosene soaked waste cotton over the bed and lighting the cotton. This was followed by supplying a known flow rate of primary air. In select experiments performed without the vessel, the secondary air holes were blocked to avoid any possible influence of that on the measurement of composition. Gas samples extracted from the stove were analysed after removal of water vapour for various components – CO, CO_2, H_2, O_2 and CH_4 using Maihak gas analyser. No hydrocarbon other than

Table 1
Mass, energy and power behavior, $\dot{m}_w$ = wood piece consumption rate.

Mode	Fuel (g)	$\dot{m}_w$ (g/min)	Cal value (MJ/kg)	Energy (MJ)	Time (min)	Power (kW)
Flaming	310	11.1	14*	4.34	28	2.6
Char	50	1.19	25	1.42	42	0.56

Biomass loaded = 360 g, Cal value = 16 MJ/kg.
* =deduced.

Table 2
Gasification A/F and char bed temperature with wood as the fuel.

$\dot{m}_{air}$ (g/min)	$\dot{m}_w$ (g/min)	A/F	T_{cb} (°C)
15	10	1.5	723
18	12	1.5	823
24	16	1.5	933

Table 3
Gas composition (volumetric) and gasification efficiency (η_g) at different wood consumption rates.

$\dot{m}_w$ (g/min)	CO (%)	CO_2 (%)	CH_4 (%)	O_2 (%)	H_2 (%)	T_g (K)	H_c (MJ/nm^3)	η_g (%)
10	8	19	1.5	2.80	1.6	1033	2.68	33
12	12.3	20	2.5	1.30	5.2	1093	3.70	47
16	13	18	2.5	0.83	7.5	1178	3.95	52

CH_4 can be measured using this gas analyser. K-type thermocouple of bead size 1 mm was used to measure the temperature of the bed. The data was acquired over the entire cycle of operation of the stove on a computer and no change in the composition of the gas analysed was taken indicative of the steady state operation of the stove.

Table 2 shows the gasification air-to-fuel ratio (A/F) and the char bed temperature measured for three different primary air mass flow rates. This simple result obtained from air-flow and fuel mass-time data confirms the known fact that the A/F of gasification is constant irrespective of the mass gasification rate in the range of flow rates considered. The char bed temperature increases with mass gasification rate. These two phenomena are consistent with the internal heat balance in the gasification process. As the air flow is increased the heat release rate will increase because more of the pyrolysis products are burnt. But this will not increase the temperature of char bed directly because the endothermic reduction reactions will aid reduction in the temperature rise. Also the amount of gas created by char bed (by reduction reactions) will increase and therefore the consumption of char will increase. This net effect results in a constant A/F even with the increase in the mass gasification rate.

Table 3 shows the gas composition and the gasification efficiency for the flaming mode operation. The composition improves with increase in the mass gasification rate. This is expected because the amount of gas reduced by char bed increases and that means more of CO_2, H_2O get converted to CO and H_2 and more tar gets cracked into simpler components.

The gasification efficiency is defined as the ratio of the energy contained in the gas at the temperature at which it is generated to the input energy in the biomass. The energy of the gas is computed by summing up the heats of formation and the sensible enthalpy of the species over their volumetric fractions. The maximum η_g obtained is 52%. However, classical downdraft gasification systems show a cold gas efficiency of 80% (hot gas efficiency ~85–87%) [17]. This discrepancy needs examination. The volume fraction of CH_4 is 2.5% but in a classical downdraft gasifier CH_4 is 1%. This indicates that the cracking of higher hydrocarbons like tar that is known to occur very effectively in a classical downdraft gasifier may not occur in a stove largely because the char bed thickness is small indeed. Even in a downdraft gasification systems, it is inferred that the fraction of higher hydrocarbons will be higher whenever CH_4 is greater than about 1%. Such a situation is therefore most likely in the stove gasification process. Since the gas analyzer used in the experiment could cannot detect it, the following strategy was adopted. The hydrogen element in the biomass can get converted into H_2, H_2O and hydrocarbons only. The volume fraction of H_2 is measured and if once the fraction of H_2O is estimated, the rest of hydrogen is inferred to be going into HC only. Assuming that the only hydrocarbon is CH_4, the amount of CH_4 equivalent in energy to other hydrocarbons can be estimated by enforcing atomic balance on the gasification reaction.

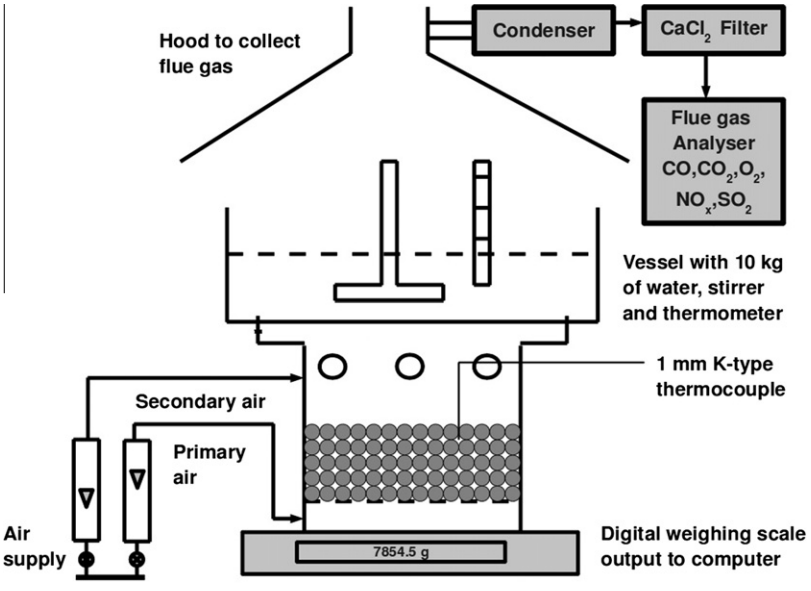

Fig. 3. Schematic of the experiment.

But to make an atomic balance, one needs to know the (a) CHNO analysis of wood, (b) A/F for gasification and (c) volume fraction of H_2O. The CHNO analysis of wood sample was outsourced to a chemical laboratory. This gave the composition as $CH_{1.72}O_{0.88}N_{0.00248}$. The A/F is known from the experiments and the volume fraction of H_2O was estimated by the experimental setup discussed earlier (Fig. 3). By measuring the amount of water condensed, the volume flow rate of gases flowing through the condenser, mass gasification rate of the biomass and the primary air volume flow rate, the volume fraction of H_2O was determined to be 10%. With these inputs the fraction of CH_4 equivalent in energy to higher hydrocarbons was determined by the following calculation.

The gasification chemical reaction is

$$CH_{1.72}O_{0.88}N_{0.00248} + x(O_2 + 3.76N_2) \rightarrow aCO + bCO_2 + cH_2 + dH_2O + eCH_4 + 3.76xN_2$$

Here e refers to CH_4 produced in the gasification reaction plus the CH_4 equivalent in energy to the other hydrocarbons. From the previous experiments we know the A/F of the gasification reaction and therefore x is known. e was calculated by solving the atomic balance equations

$$C : a + b + e = 1 \quad (1)$$

$$H : 2c + 2d + 4e = 1.72 \quad (2)$$

$$O : a + 2b + d = 0.88 + 2x \quad (3)$$

We have three equations and five unknowns. But from experiment we know the volume fraction of CO, CO_2 on dry basis and this gives the following two equations.

$$a/(a + b + c + e + 3.76x) = 0.13 \quad (4)$$

$$b/(a + b + c + e + 3.76x) = 0.19 \quad (5)$$

Using these, the atomic balance equations were solved. The final composition along with the gasification efficiency is shown in Table 4.

3. Simulation of gas phase combustion and heat transfer

The flaming mode efficiency η'_{fla} of the stove is the ratio of the heat transferred to the vessel to the energy put into the stove in the flaming mode. This is a product of the gasification efficiency η_g and the convective heat transfer efficiency η_{con} from the gas phase combustion to the vessel (the heat transfer by radiation from the stove wall to the vessel is included in this). Apart from this, the hot char bed transfers heat to the vessel by radiation and this efficiency is denoted by η_{rad}.

$$\eta'_f = \eta_g \eta_{con} + \eta_{rad} \quad (6)$$

The next step is to determine the convective heat transfer efficiency (η_{con}). The convective heat transfer to the vessel was determined by simulating the gas phase combustion process in the stove. For this the conservation equations for reacting flow with appropriate boundary condition were solved.

In order to simulate the flow in a stove it is required to know whether the flow is laminar or turbulent. The stove is essentially a cylinder of diameter 100 mm and 18 circular jets on its circumference. Average biomass burn rate is 13 g/min and the stoichiometric A/F is 4.9. Therefore for stoichiometric operation, total flow through the stove is 76.7 g/min. The flow Reynolds number with the stove diameter (100 mm) as the characteristic length is $Re_d = \rho Vd/\mu = 4\ m/\pi d\mu = 301.4$. This is very small compared to Re_{crit} (for transition to turbulent flow) for flow through a cylindrical duct constituting the combustion chamber. But there are 18 jets coming into the cross-flow and the critical Reynolds number of jet is small. Reynolds number based on jet diameter and the mass flow of secondary air is $Re_{d_j} = \rho Vd/\mu = 4\dot{m}_{air}/\pi d\mu = 391$. Even if at this Reynolds number, the jet could be turbulent. But the jets are issuing into a chamber that has a high viscosity (due to high temperatures in the combustion chamber). The net behavior is close to laminar flow – the physical appearance is of a mildly dancing diffusion flame.

In actual stove the secondary air is supplied using a fan which blows air into a plenum and then it enters the combustion chamber through 18 circular holes on the circumference of the chamber. Issues of axi-symmetry and nature of inflow velocity profile were settled by simulating the cold flow through the plenum and the stove combustion chamber.

The flow domain used for the calculation is shown in Fig. 4. Structured grid with 0.15 million cells was used to compute the flow field using ANSYS-CFX commercial code. Mass inlet boundary condition for the main inlet, zero pressure gradient for the outlet and no slip no penetration boundary condition for the walls was used. The results are presented in Fig. 5.

There is some asymmetry in the velocity profile but does not appear significant. Since we are interested in overall thermal behaviour, a symmetric parabolic profile was taken to approximate the velocity profile and the simulations were performed. For the ease of computation a 20° sector with one secondary air inlet was simulated assuming symmetry and a parabolic velocity profile was assumed for air inlets. The computational domain along with the boundary conditions used are shown in Fig. 6.

The flame in the stove is non-premixed and therefore the chemical reactions were assumed to be mixing controlled. The calculations were made with additional transport equation for the mixture fraction and algebraic equation for mass fractions of various components. Heat transfer due to radiation from the gases and the stove walls was modelled using discreet transfer equations.

A few preliminary computations showed that the stagnation boundary layer at the bottom of the vessel requires a fine grid. Capturing this with good resolution is crucial because the aim of the computation is to determine the vessel wall temperature gradient. The wall heat flux along the bottom of the vessel is shown for three different grids in Fig. 7. A grid with 0.26 million nodes (220 mm diameter vessel) and 0.2 mm size in the direction normal to the vessel wall resolved the boundary layer with sufficient accuracy. The point to note is that the coarse grid had problems resolving

Table 4
Composition corrected using atomic balance.

$\dot{m}_w$ (g/min)	CO (%)	CO_2 (%)	CH_4 (%)	O_2 (%)	H_2 (%)	H_2O (%)	η_g (%)
16	14.3	14.1	5.2	1.2	9.3	10	80

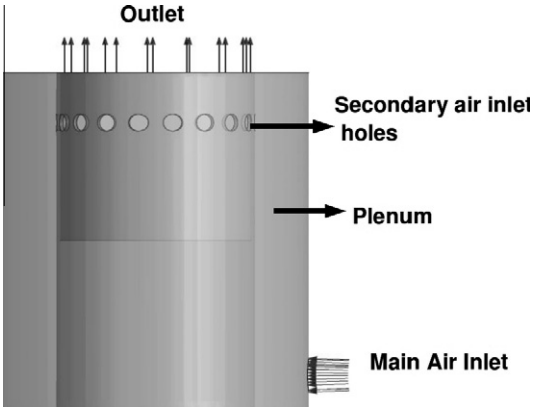

Fig. 4. Computational domain for calculating secondary air distribution.

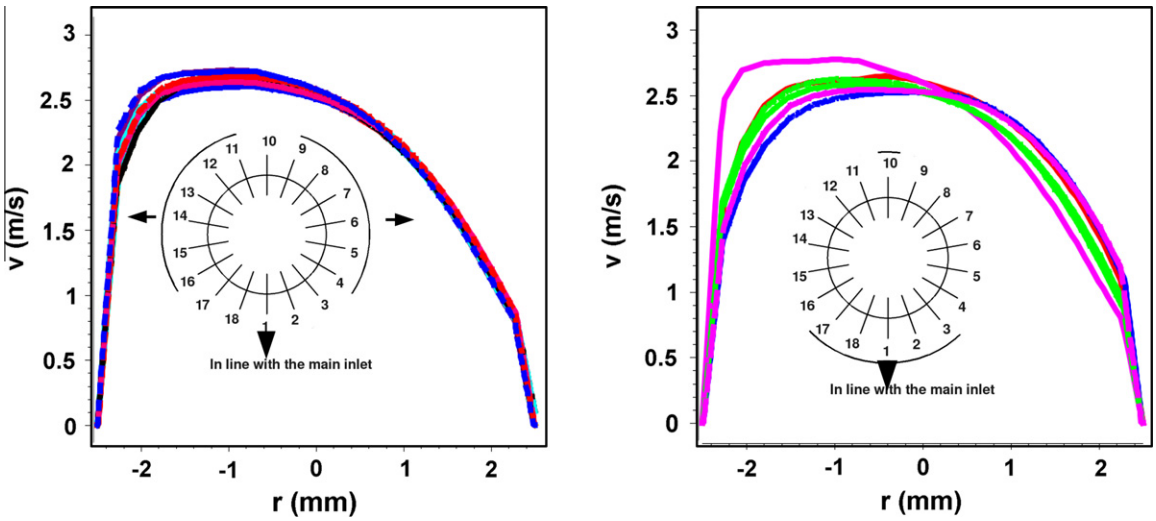

Fig. 5. Secondary air inlet velocity profile.

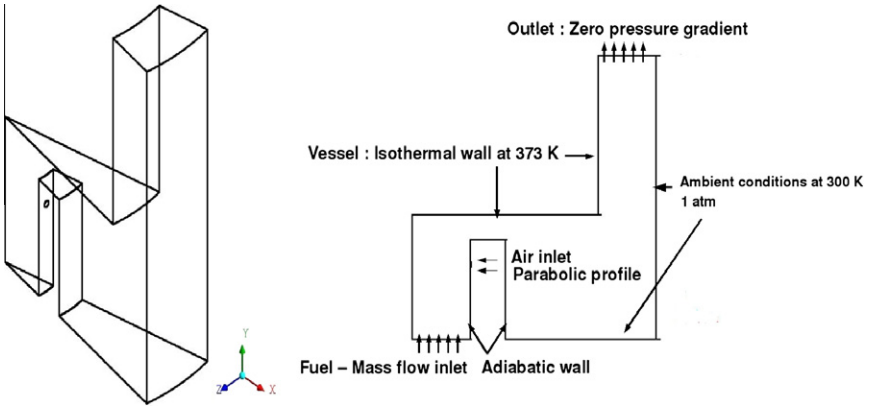

Fig. 6. Computational domain and boundary conditions.

the flow features close to the stagnation point. It was found that this would not affect the prediction of total heat transfer, because of very small area close to the stagnation point.

Grid independent stagnation point boundary layer profiles are shown in Fig. 8 for different points along the vessel wall. It is clear from the plot that the gradients are strong within 1–2 mm from the wall and decrease as we move away from the stagnation point along the vessel wall. Therefore the heat flux is maximum near the stagnation point.

The total heat transfer to the vessel up to radius r is given by Eq. (7). Fig. 9 shows the wall heat flux, the area of the vessel and the heat transferred to the vessel up to radius r as a function of radius of the vessel.

$$\dot{q} = \int_0^r \dot{q}'' 2\pi r dr \tag{7}$$

Once the quantity $\dot{q}''$ is obtained the convective heat transfer efficiency can be obtained. The heat transferred to the vessel side wall was included into $\dot{q}$ for calculating η_{con}. Computations were performed for vessels of 220, 260 and 320 mm diameter that are the kind of dimensions of practical cooking vessels. Table 5 presents the results of the computations.

The results clearly indicate better utilization of heat as the vessel size is increased. Introducing swirl is sometimes claimed to enhance the heat transfer to the vessel. Calculations done with

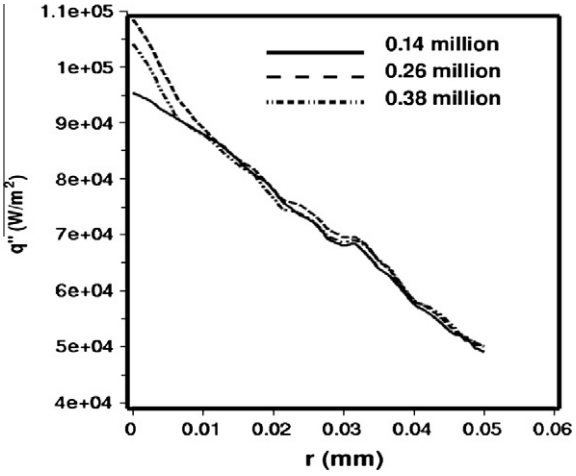

Fig. 7. Grid independence test.

30° showed marginal changes in the heat flux along the radius and on integration, the heat transferred to the vessel seemed unaffected by the swirl.

From here we are just one step away (heat transfer due to radiation from char bed) from determining the overall efficiency of the stove. The methodology used to determine η_{rad} is explained below.

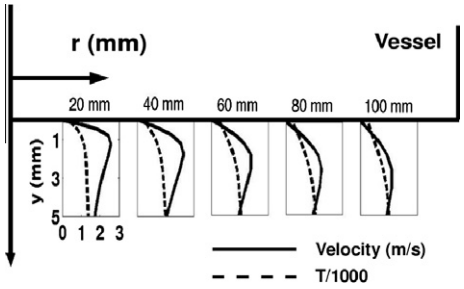

Fig. 8. Stagnation point boundary layer profile.

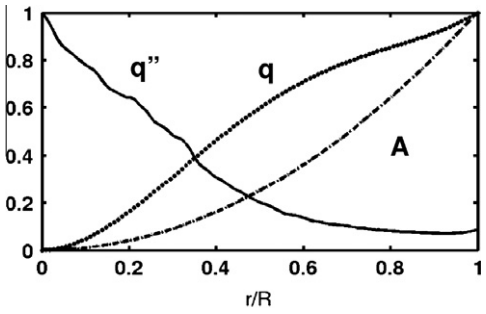

Fig. 9. The variation of heat transfer along the radius of the vessel.

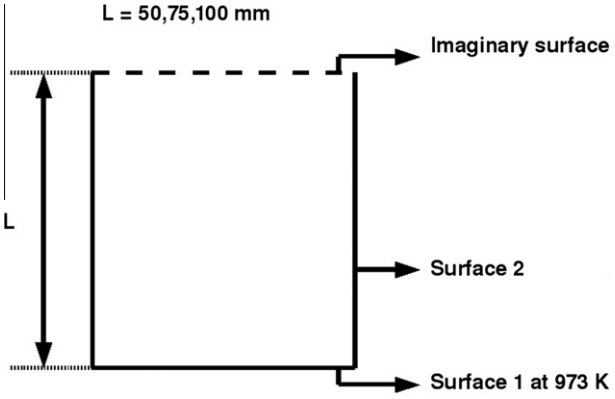

Fig. 10. Model for theoretical prediction.

Table 6
View factors.

L (mm)	F13
50	0.38
75	0.25
100	0.20

Table 5
Efficiency.

d_v (mm)	η_{con} (%)
220	52.8
260	58.0
320	65.2

Table 7
Radiative heat transfer.

L (mm)	q_R (W)
50	167
75	110
100	90

3.1. Radiation heat transfer efficiency (η_{rad})

The heat transfer from the hot char bed to the vessel was determined theoretically. The geometry used in the calculation is shown in Fig. 10.

To estimate the radiative heat transfer to the vessel from the char bed, the fraction of energy emitted by surface 1 intercepted by imaginary surface 3 is to be calculated. For this, the view factor F13 is required. For this geometry the view factors are known from standard charts [18] and is shown in Table 6.

Char was assumed to be a blackbody at 1000 K. The theoretical radiative flux intercepted by surface 3 was calculated using (8).

$$q_r = 5.67e-8 \times 1 \times A1 \times F13 \times (1000^4 - 343^4) \quad (8)$$

Since the depth at which the char bed exists changes as the stove operates calculations were done for three different depths and the average was taken as the contribution of radiation from the char bed. The results are set out in Table 7.

Average heat transfer rate is 122 W. This theoretical estimate was put to test using experiments. The experimental setup is very similar to the one shown in Fig. 3, but instead of biomass loaded in the chamber, the chamber was sealed and evacuated using a vacuum pump to 550 mm of Hg below atmosphere. The base plate was maintained at about 1000 K and the heat transferred to the water was calculated as before. The measured heat transfer rate was 160 W. This is slightly higher than the average number estimated from the theory. In experiments there is a possibility of other modes of heat transfer like natural convection and conduction (because of direct contact). Taking into account these factors the measured values are not very far from the theoretical values. Therefore from combination of experiments and theory the contribution of radiation to efficiency is about 6 ± 1%.

Table 8
Overall efficiency.

d_v (mm)	η_g (%)	η_{con} (%)	η_{rad} (%)	η'_{fla} (%)
220	80	52.8	6.0	48.3
260	80	58.0	6.0	52.4
320	80	65.2	6.0	58.2

Now that all the components of the efficiency are determined, the overall efficiency picture is as shown in Table 8.

The experiments and computations lead to the following important features of the stove operation.

1. The products of gasification from a reverse downdraft system contains more uncracked higher hydrocarbons compared to a classical downdraft system and a simple method to calculate the fraction of HHC was devised. Application of that method showed that the gasification efficiency of a stove is same as that of a gasifier.
2. The dependence of convective heat transfer efficiency on the vessel size has been brought out.
3. Contribution of radiative heat transfer from char bed to efficiency is 6 ± 1%.

Table 9
Vessel size effect – experiment and CFD.

d_v (mm)	η'_{fla} Experiment* (%)	η'_{fla} CFD (%)
220	49 ± 2	48
260	52 ± 2	52
320	55 ± 2	58

* Calorific value of biomass 16 ± 0.5 MJ/kg

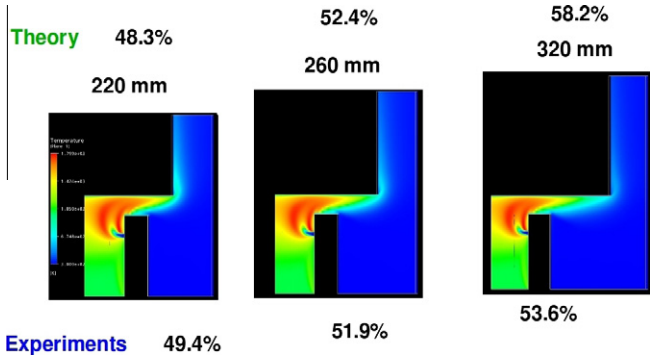

Fig. 11. Effect of vessel size on heat extraction.

4. Vessel size effects – Experiments and computations

Table 9 shows the effect of vessel size on efficiency determined from experiments and simulation. The fair comparison between the experiments and calculations (see Fig. 11) brings out the point that using vessels of appropriate size is crucial to improving the utilization efficiency. It is clear from Fig. 11 that as the vessel size is increased more and more of heat is extracted from the hot product gases leaving the stove. The efficiency will keep increasing with the diameter till a stage when the heat loss from the sides becomes significant.

5. Conclusions

The components of the efficiency of the stove are clearly established with experiments and simulations. The energy equivalent of higher hydrocarbons is determined using experiments and atomic balance to be 5.5% CH_4 and is used to establish the similarity between stove and classical gasifier in terms of gasification efficiency. The simulation of gas phase reactions and heat transfer in the stove showed that (a) the calculated data compare well with the experimental data, (b) the heat extraction is a strong function of the vessel size with efficiency increasing with the diameter of the vessel and (c) swirl has negligible effect on the heat transfer. The radiation from the char bed to the vessel is shown to contribute about 6 ± 1% to the efficiency.

The insights obtained in this work and an associated paper of the authors [11] have been used to enhance the efficiency and reduce the emissions of not only domestic stoves but larger size commercial stoves meant for community cooking.

References

[1] Kaupp A. Gasification of rice hulls: theory and praxis. GATE/GTZ. Eschborn. DE; 1984.
[2] Mukunda H, Dasappa S, Paul P, Rajan N, Yagnaraman M, Kumar D, et al. technology and field outreach. Curr Sci 2010;98(5):627.
[3] Reed T, Larson R. A wood–gas stove for developing countries. Energy Sustain Dev 1996;3(2):34–7.
[4] Reed T, Anselmoa E, Kircherc K. Testing & modeling the wood–gas turbo stove. In: Progress in thermochemical biomass conversion. Conference, September 17–22, Tyrol Austria; 2000.
[5] Balat M, Balat M, Kirtay E, Balat H. Main routes for the thermo-conversion of biomass into fuels and chemicals. Part 2: Gasification systems. Energy Convers Manag 2009;50(12):3158–68.
[6] Zhang L, Xu C, Champagne P. Overview of recent advances in thermo-chemical conversion of biomass. Energy Convers Manag 2010;51(5):969–82.
[7] Fatehi M, Kaviany M. Adiabatic reverse combustion in a packed bed. Combust Flame 1994;99:1–17.
[8] Harttanainen M, Saastamoinen J, Sarkomaa P. Operational limits of ignition front propagation against airflow in packed beds of different wood fuels. Energy Fuels 2002;16:676–86.
[9] Porteiro J, Patino D, Moran J, Granada E. Study of a fixed-bed biomass combustor: influential parameters on ignition front propagation using parametric analysis. Energy Fuels 24.
[10] Gort R, Brouwers JJH. Theoretical analysis of the propagation of a reaction front in a packed bed. Combust Flame 2001;124:1–13.
[11] Ronnback M, Axell M, Gustavsson L, Thunman H, Leckner B. Combustion processes in a biomass fuel bed – experimental results. Prog Thermochem Biomass Convers 2001:743–57.
[12] Reed T, Walt R, Ellis S, Das A, Deutch S. Superficial velocity – the key to downdraft gasification. In: Fourth biomass conference of the Americas, Oakland, USA; 1999. p. 343–56.
[13] Mukunda HS. Understanding clean energy and fuels from biomass. 1st ed. Wiley; 2011.
[14] Varunkumar S, Rajan NKS, Mukunda HS. Studies on a gasifier stove. Energy Sustain Dev.
[15] La Fontaine H, Reed T. An inverted downdraft wood–gas stove and charcoal producer, Washington, DC.
[16] Varunkumar S, Rajan NKS, Mukunda HS. Single particle and packed bed combustion in modern gasifier stoves – density effects. Combust Sci Technol. 2011;183(11).
[17] Mukunda HS, Dasappa S, Paul PJ, Rajan NKS, Shrinivasa U, Sridhar G, et al. Fixed bed gasification for electricity generation, biomass gasification and pyrolysis, state of the art and future prospects. Tech. rep., European Commission 1997.
[18] Incropera, Dewitt. Fundamentals of heat and mass transfer. Wiley; 1996.